Fermi National Accelerator Laboratory

FERMILAB-TM-1733

Radiation Shielding Tests in the Meson Beamline in the Master Substation Area

R. Coleman, W. Kissel, A. Leveling, C. D. Moore, and V. Vylet
Fermi National Accelerator Laboratory
P.O. Box 500
Batavia, Illinois 60510

April 1991

Operated by Universities Research Association Inc. under contract with the United States Department of Energy

Radiation Shielding Tests in the Meson Beamline in the Master Substation Area

R. Coleman, W. Kissel, A. Leveling, C. D. Moore, and V. Vylet

A review of shielding uncovered a weak region in a portion of the proton beam transport to the Meson Area. Preliminary CASIM Monte Carlo studies indicated dose rates at the surface under abnormal operating conditions would be above the Fermilab Radiation Guide limits. Measurements made on December 15 and 16 confirmed this concern. Further comparisons of data with CASIM predictions are discussed.

Introduction

During the course of a routine study of the shielding requirements for the Main Injector upgrade, a potential weak region was discovered even for current intensities. A plan view of the region around the master substation is shown in Figure 1 with regions of detailed studies indicated. An elevation view of the area is given in Figure 2, and the first indication that there may be a problem is immediately obvious; there is an access road to the north of the substation fence which travels over the beamline after the heavy concrete shielding has stopped and before the berm starts rising. Additional concerns were raised about the amount of earth cover in the substation yard itself, even with the presence of heavy concrete. Finally, there appeared to be some minor difficulties upstream of the substation with respect to having this area unposted.

A new survey technique which analyzed aerial photographs of the site and produced ground level contours along a beam line was used to verify the problem. In Figure 2 a double check using this procedure is shown for the region of the substation yard; the agreement is very good ranging from .2 foot to .6 foot. The quoted level of accuracy from the company[1], for a region not obscured by vegetation, is ±0.5 foot 90% of the time, and hence we see in this region they are well within their quoted errors.

The thinness of the earth shield would be less of a problem if it were not possible to directly dump beam in the buried berm pipe. Figures 3 and 4 show aperture restrictions in the Meson line in the region of concern. In addition to the apertures shown in Figures 3 and 4, two beam position monitors (BPM) are located just upstream of M00H in F2. Each BPM is 1 meter long and has cylindrical copper plates 2.625" in diameter and 0.0625" in thickness. A visual inspection of the flanging at the entrance and exit points in F2 and F3 suggests that the berm pipe is not perfectly aligned. In addition, beam scans and optical scans documented in Switchyard logbooks[2], and communications with past members of the Switchyard Department[3] indicate that there were problems with getting the beam through due to a pipe misalignment of magnitude such that there was only 5" of clear aperture out of 10". Another piece of information available is a videotape made by pulling a tv camera through the berm pipe. This videotape indicates that there are no obstructions such as conduit or lead bricks on the bottom of the pipe from F2 to F3 which could act as targets. There are rocks present on the bottom and there are the "chill rings" associated with the welding process. These however would present small fractions of an interaction length to the beam. A recent survey of the vertical profile of the 10" pipe done after these radiation tests is shown in Figure 4. Horizontally the pipe was much straighter (±0.8"), however the beam is offset with respect to the pipe as indicated in Figure 3.

This information was used to generate a source term for Monte Carlo (CASIM[4]) studies of beam loss in the beam pipe. These studies indicated that dose rates at the surface would be larger if beam were lost on the top of the pipe rather than at the bottom with a grazing incidence. Since we knew that there were no targets on the bottom or abrupt changes in the pipe, the CASIM runs with a grazing incidence at the top were taken as worst cases. These runs indicated that in fact dose rates would be above the Fermilab Radiation Guide limits under accident conditions.

An aspect of the situation which made matters awkward was the 345 kV lines in the substation yard. There were concerns about meeting the relevant codes concerning the distance between ground and the high voltage lines if the required berm was too high, along with the practical concern of operating machinery in the yard. These concerns along with the possibility that we could not directly hit

the berm pipe made a study period desirable to actually measure the above ground dose under accident conditions.

Hence a study period was scheduled for December 15-16, 1990 during daylight hours. The reason for the specification of daylight hours was to ensure security of an area that was nominally open to public access. A tremendous amount of cooperation between the Business Services Section, Research Division, and the Accelerator Division ensured that the tests were carried out in a prudent and safe manner. The entire outer region was blocked off with site security's assistance and an inner exclusion area was defined with ropes. No one was permitted inside this inner area unless the local area safety coordinator had a key in his possession which precluded beam from the Meson line. In addition, the Main Control Room (MCR) crew chief had to have verbal authorization from the local area safety coordinator to send beam down the Meson line. This authorization was given after visual inspection of the test area and checking with a security guard who was posted on top of the neutrino berm. Another precaution taken was to limit the number of Booster batches to one (about 0.9 E12 protons per 20 second spill). This limit was enforced by limiting the consoles that could change the number of batches to those in the MCR via a software change and then imposing administrative control.

One important preparation for this experiment was the installation of chipmunks (radiation monitors with tissue equivalent chambers) as depicted on Figure 2. Both power and signal cables were run to the detectors enclosed in portable wooden sheds (doghouses). There were 10 detectors and 8 channels available for readback purposes. These 8 channels were logged along with other pertinent information such as magnet currents, intensities, and loss monitors. Having this information available proved valuable in analyzing the data. (The loss monitor data was logged successfully only on the second day of the test; however, it was available in the MCR in the usual way throughout the test.) The 8 channels were recorded in a redundant manner by both the Research and Accelerator Divisions.

This was the first attempt to deliver beam to the Meson area in several months. Beam had been sent to the Switchyard dump and extraction was tuned up previously so a good base had been established, and beam was delivered to the Meson train relatively quickly.

There were four parts to the tests:

1. Beam loss upstream of F2
2. Beam loss downstream of F2
3. Beam loss on beam valve in F2 (downstream)
4. Beam loss on magnet in F2

The general idea of the first two parts is very simple; try to hit the berm pipe on the top (worst case from CASIM) and if successful, map out the loss in detail using portable instruments. If not successful, try bending horizontally to hit the side of the pipe. The purpose of the beam valve experiment was to have a very controlled source term for purposes of comparing the experimental results to CASIM. Finally the beam loss on a magnet in F2 was intended to be a repeat of an earlier experiment[5].

12/15/90 Data from (mainly) Upstream of F2

The marshalling of effort for the experiment started around 0600 with the placement of barricades and ropes in the substation area. Beam was sent to the Switchyard dump at 0914 and after further safety system checkout by the Research Division and Accelerator Division safety groups, the critical devices for the Meson area were unlocked. Beam to Meson was established by 1230.

For this experiment, detector 9 (physically on the road north of the substation) was on channel 8 of the readback system, and detector 0 (physically located on the side of road A) was on channel 1 of the readback system. The experiment started by lowering the current in magnet V210, which is a downward bending magnet. This is shown in Figure A of the Appendix which includes the effect of the kick due to the septa (FSEP) and the finite size of the beam. While the emphasis on the first day was to maximize the radiation upstream of F2, Figure 5 shows an interesting loss pattern which we now understand is due to the beam hitting the plate of the BPM and also hitting a misaligned gate valve as indicated in Figure A. Figure 6 shows the response of detector 0 as V210 was varied and Table A shows the corresponding pattern of the other detectors. Figure 6 indicates that we were hitting the berm pipe and were able to make a maximum dose rate appear at the detector.

In order to verify the peak and to gain more information, two fine-grained scans were performed using portable HP1010 instruments. Both of these detailed scans used a 5' spacing between the detectors with one of the HP1010 detectors at the same location as the chipmunk. Having one of the detectors at the same location as the chipmunk allowed us to have an independent check of our remote monitoring system. Figure 7 shows the finer grained longitudinal scan and indeed showed that we were able to position the shower maximum at roughly the chipmunk location. In Figure 8 we show the transverse scan and the fact that the peak was at the chipmunk was an independent verification of the surveyor's line.

Also shown in Figures 7 and 8 are the CASIM predictions. The model assumed the beam hit the top of the 8" diameter pipe upstream of the F2 enclosure with a grazing angle (~2 mr). The CASIM results are about twice the measurements.

12/16/90 Data from F2 and Downstream of F2

For the remaining tests, detector 9 was still in channel 8, but detector 1 was in channel 1 of the readback system. As mentioned above, our first goal was to attempt to hit the berm pipe north of F2 on the top in order to maximize losses above ground (see Figure B). We were able to steadily increase the reading on the last detector and Figure 9 shows the radiation pattern through the yard with the maximum current of M00V equal to 175 amps. After the experiment was over, we investigated the alignment of the pipe downstream of F2 and noticed that there was a vertical sag by the beam valve in the downstream end of the enclosure. An indication that some scraping was occurring is evident from the significant increase in the readings from detectors 2 and 3 given in Table B.

We had been able to achieve a nice peak reading upstream of F2 and our goal here was to first maximize the reading on the detector on the road north of the substation, then to try to move the peak south inside the substation yard. From Figure 4 one can see that we can get a larger angle for the ray by lowering the beam in F1 and raising the beam in F2. We tried this in two stages; first we raised the beam in F2 using magnet V210 while keeping M00V at its high value. The results are given in Table C along with the loss monitor information which became available at this time. The loss monitors recorded were: F2US(DS) and F3US(DS) located at the entrance (exit)

berm pipes in F2 and F3 enclosures and loss monitors located on the dipoles in F2 and F3. An interpretation of the pattern of readings given in Table C follows:

1.	V210=202	The beam is scraping in downstream F2
2.	V210=192	The beam is hitting the vertical BPM plates.
3.	V210=182	The beam is above the BPM plates but not yet directly hitting M00H, also the beam is pointing close to detector 9.
4.	V210=162	The beam is dumping in M00H.

Figure 10 shows the detector pattern when the reading at the road is the highest.

The next step involved trying a possibly even larger angle by dropping the beam in F1, and raising the beam in F2, again with M00V set high (Figure D). Figure 11 gives the detector pattern with the maximum loss at the road. At this point we wanted to make a more detailed scan to try to determine the shape around the high dose rate at the road. Figure 12 gives this more detailed distribution from the HP1010's. Note that the falloff downstream of detector 9 is due in part or altogether to the increased berm height. The distribution upstream may also reflect the heavy concrete shielding that is in place inside the yard. Unfortunately unlike the measurements made on the previous day, the handheld HP1010 is about one-half the value measured by the chipmunk detectors at the peak of the distribution comparing Figures 11 and 12.

Since we were never able to move a peak reading to detector 7 by any means vertically we proceded to try horizontally. Again as a first step we simply used M00H, but kept M00V pointed high in order to maximize the above ground losses (Figure E). We were able to increase the losses at the road by swinging the beam to the east. This is the direction we thought would be best for causing losses due to the pattern of the flanges in F3. Figure 13 shows the pattern with the maximum loss on detector 9.

Next M00H was restored to its nominal setting, beam was positioned to the west in F1, and then H210 was used to do a horizontal scan from west to east. Figure F clearly indicates that the beam should have passed cleanly through F2, however loss

monitor F2DS indicated that we were scraping on something. Also the ratio of detector 9 to detector 2 is roughly constant, shown in Table F, which indicates that we were not shining directly on detector 9 but rather scraping in F2 and sending interaction products down the pipe. Figure 14 shows the loss pattern at the maximum reading on detector 9.

Next we did a M00H scan to the east (Figure G). The ratio of detector 9 to detector 2 (Table G) increases from about 3 to 5 indicating that we were hitting the berm pipe between F2 and F3 upstream of detector 9 for the first time. Figure 15 gives the loss pattern at the condition of maximum loss on detector 9. We then made a transverse scan at this condition (except for M00H which had to be turned down due to overtemperature trips) and the results are shown in Figure 16. The peak of the distribution was where the surveyors had indicated, however the handheld detectors read about one-half of the fixed chipmunk detectors in the peak.

Figure 17 shows the similarity of many of the loss patterns observed in the remote detectors. The common factor for the beam trajectories through F2 was the high vertical position in downstream F2, while the beam angles varied considerably. A CASIM calculation was done to simulate this common loss pattern. It included the dirt and heavy concrete shielding, the vertical misalignment of the gate value and neighboring 4" beam pipe, an approximation to the surveyed vertical positions of the 10" pipe between F2 and F3, and the proper 800 GeV/c beam spot size. With these assumptions all of the beam passed through 1.5" of aluminum at the gate valve. Figure 18 shows the results.

Note that in Figure 17 the maximum rate observed in detector 9 occurs in data from Table G where we were likely hitting the berm pipe upstream of detector 9. CASIM calculations show peak levels of 1 to 3 mrem per pulse at detector 9 from the beam directly striking the berm pipe upstream of detector 9.

In conclusion the possible accident radiation levels in the substation and areas upstream and downstream of it were above those permitted by the Fermilab Radiation Guide for current amounts of shielding and level of posting.

Beam Valve Closure Test

One problem that occurs very frequently in situations like this is knowing exactly what the source term is for CASIM, i.e. the exact details of the loss. Hence, a very controlled loss mechanism was used; a beam valve in the downstream end of F2 was closed and beam was run into the valve. As Table H indicates we were going into and through F2 very cleanly. One observation is the low reading on F2DS loss monitor. This loss monitor was about 2' downstream of the loss point and half a foot transverse to the beam. The longitudinal loss pattern is shown in Figure 19 and it is interesting that the pattern is very similar to others that were observed in this experiment; although the small readings are very close to background (beam on, nominal tune) which ranged from 0 to 1 count. For this measurement we have a CASIM result which is two orders of magnitude smaller than the measurement. We do not understand the source of this discrepancy. The radiation level is the smallest of the measurements we made. It is possible that some small beam scraping upstream of the gate valve went unnoticed in the two pulses devoted to this experiment. A repeat of the experiment would be desirable to resolve the discrepancy. It would also be informative to do the experiment with a thicker target and hence larger levels of radiation as a check.

We placed the handheld monitors for a transverse scan perpendicular to detector 2. The reason for this choice of longitudinal origin was that we were able to map out the ditch that runs parallel to road A1. Figure 20 gives the readings and the peak reading is disturbingly large. The high readings are in the ditch but there is still too much transverse dirt between the bermpipe and the ditch. One speculation is that the culvert is transmitting neutrons so that the reading in the ditch is not only due to the cascade at the ditch but from a buildup upstream which allows the culvert to funnel neutrons down the ditch. Another possibility is that the handheld monitor was not reset properly.

Beam Loss on Magnet in F2

A reason for the existence of the culvert is an earlier study[5] of the radiation levels resulting from losses in F2. We attempted to replicate that experiment by dumping beam on a magnet in the middle of F2. We did this by raising the beam in F2 so that we would hit M00H. As shown in Table H the beam came cleanly into F2 and

dumped in F2. Figure 21 shows the longitudinal loss pattern in this case. However, we had placed the handheld instruments around detector 1 in such a manner as to map out the cascade, in particular we tried to have 2 detectors upstream of the peak. Clearly we did not succeed. We believe the reason is that BPM's have been added since the earlier experiment and we were starting to hit on the plates of the vertical BPM. The results of detailed CASIM modeling this hypothesis is shown in Figure 22. The agreement is reasonable in magnitude but shifted somewhat longitudinally.

References

1. Aero-metric Engineering, PO 449, Sheboygan, Wisc. 53082.

2. Switchyard Log November,1983.

3. Sam Childress, private communication.

4. A. Van Ginneken and M. Awschalom, High Energy Particle Interactions in Large Targets (1975), Fermi National Accelerator Laboratory, Batavia, Illinois, USA; and A. Van Ginneken, Fermilab Report FN-272 (1975), Fermi National Accelerator Laboratory, Batavia, Illinois, USA.

5. Peder Yurista, private communication.

List of Figures

Introduction

12/15/90 Data from (mainly) Upstream of F2

Detector 9 is in channel 8 of the readback
Detector 0 is in channel 1 of the readback and is physically located at the side of road A.

12/16/90 Data from F2 and Downstream of F2

Detector 1 is in channel 1
Detector 9 is still in channel 8

Vertical

Figure 9. Stationary detector profile using only M00V to maximize losses.

Figure 10. Detector profile raising the beam in F2 and using M00V to maximize losses.

Figure 11. Detector profile lowering the beam in F1, raising the beam in F2 and using M00V to maximize losses.

Figure 12. Detailed longitudinal profile around detector 9 using HP1010's. Note that the falloff downstream of #9 is due in part, or altogether, to the increased berm height.

Horizontal

Figure 13. Detector profile using M00H to maximize losses (keeping M00V high).

Figure 14. Detector profile moving beam to the west in F1 (until losses), moving beam to east in F2 (until losses) with M00H at nominal setting.

Figure 15. Detector profile with conditions same as for Figure 14 except M00H changed polarity and was swept to maximize loss.

Figure 16. Detailed transverse profile using HP1010's with conditions almost as in Figure 15. M00H had to be turned down to 175 amps due to over temperature trips.

Figure 17. Summary of loss patterns observed.

Figure 18. Comparison of common loss pattern observed and CASIM Monte Carlo predictions.

Beam valve closure test

Figure 19. Detector profile with beam valve in downstream F2 closed.

Figure 20. Detailed transverse scan using portable HP1010's. The maximum occurs at the bottom of the drainage ditch.

Dumping beam in the middle of F2 test

Figure 21. Stationary detector profile dumping beam in M00H.

Figure 22. Detailed longitudinal profile using HP1010's when beam is dumped in M00H.

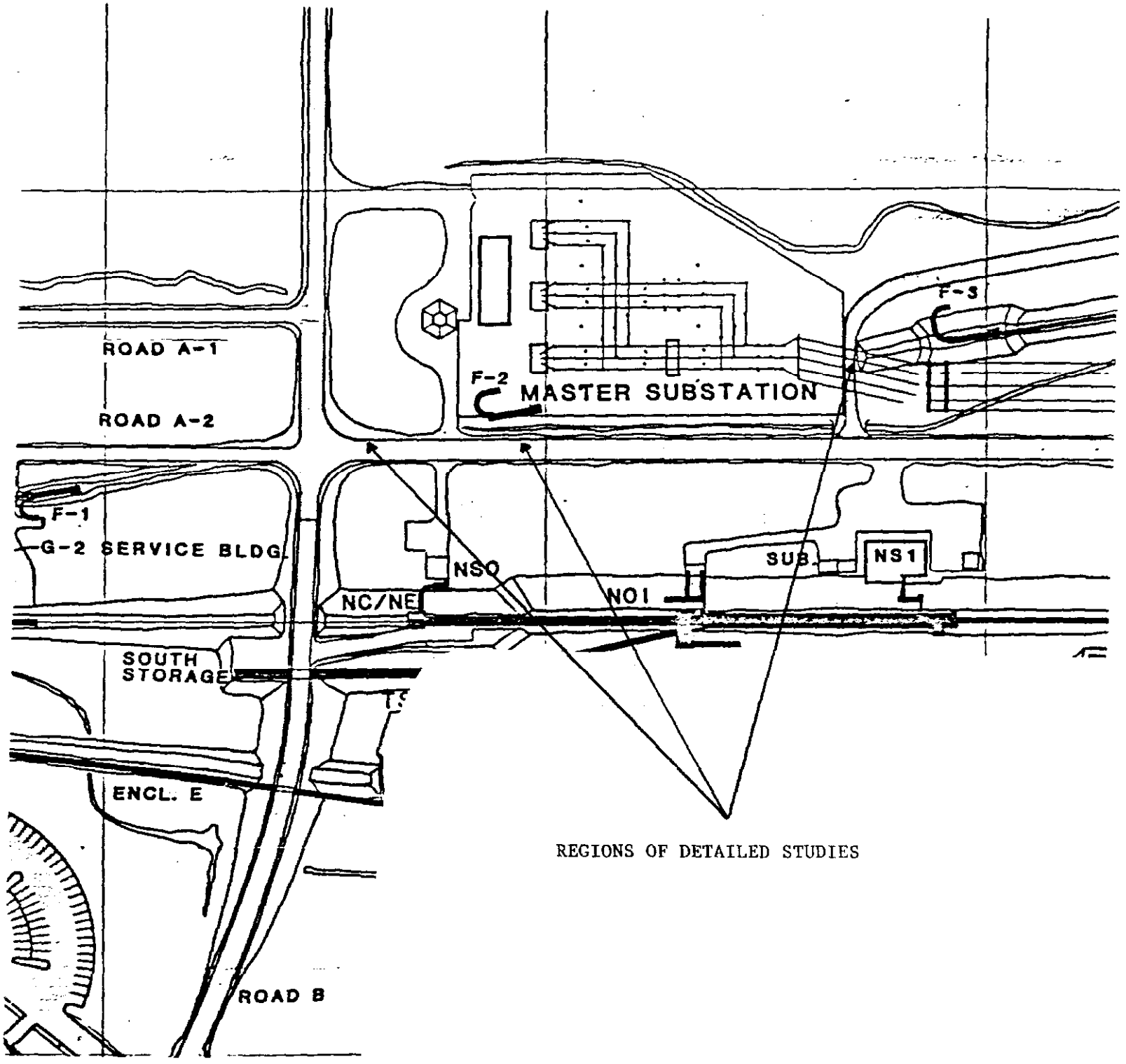

FIGURE 1
PLAN VIEW OF SUBSTATION AREA

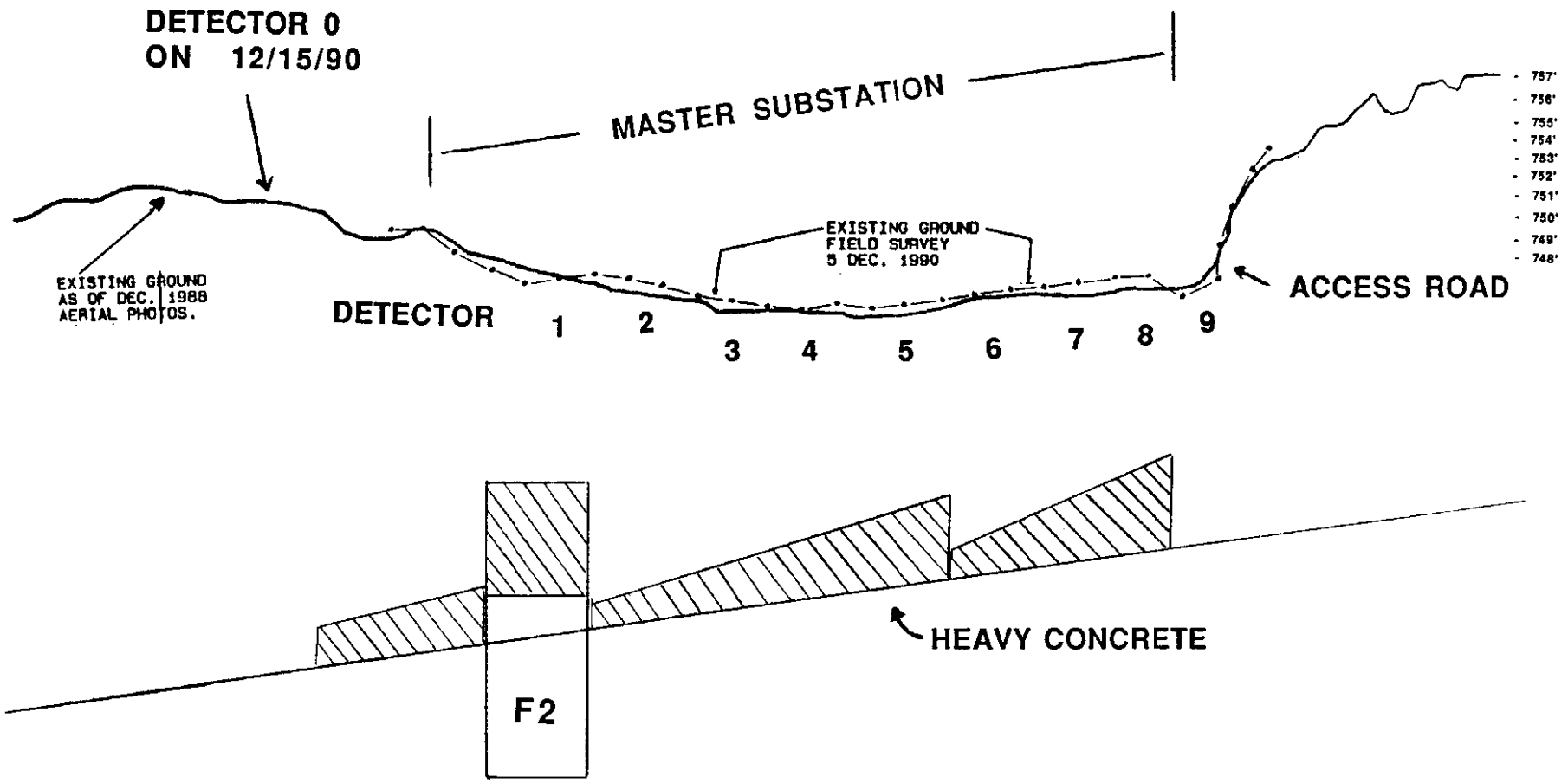

FIGURE 2
ELEVATION VIEW OF
MASTER SUBSTATION AREA

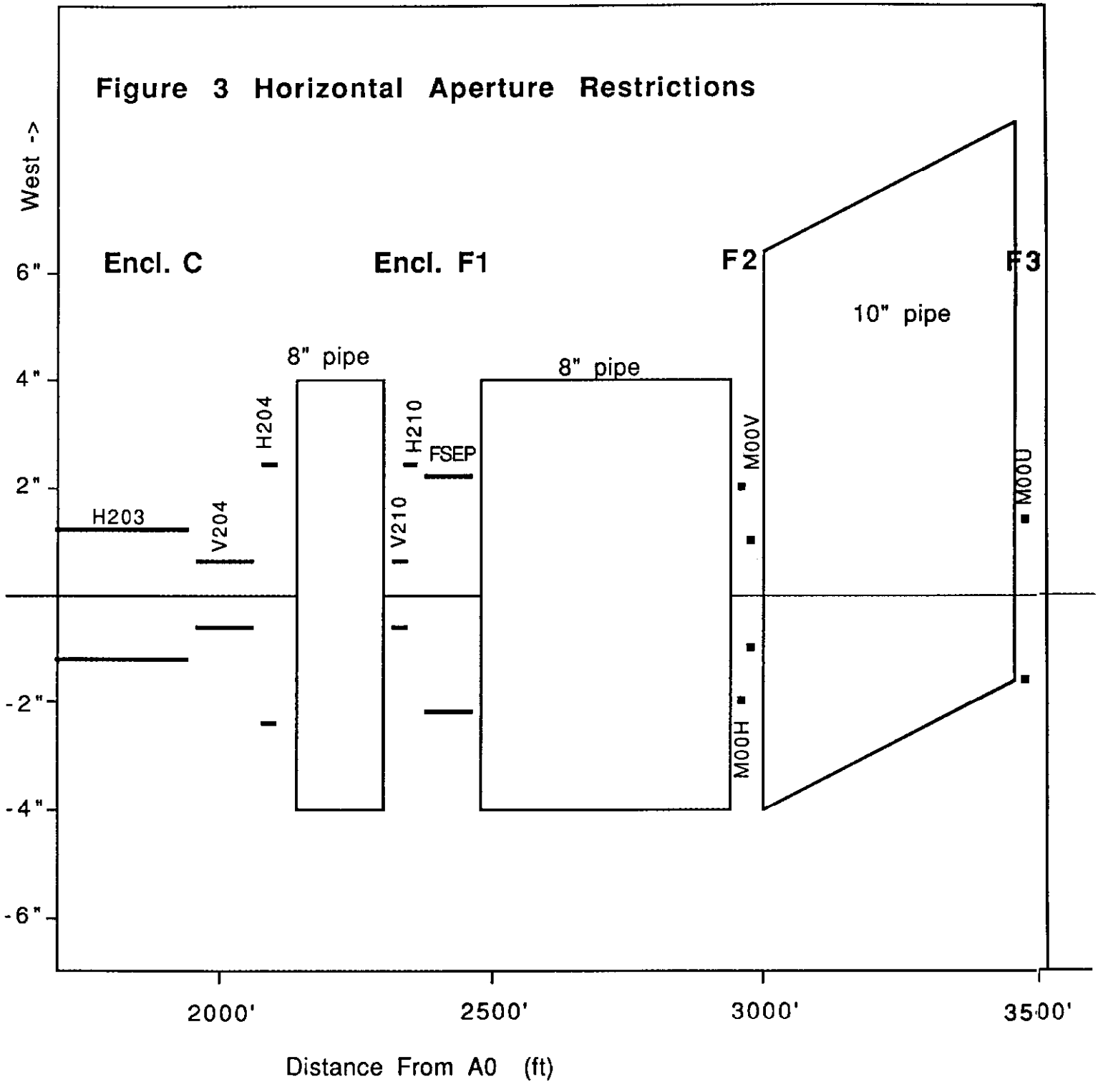
Figure 3 Horizontal Aperture Restrictions
West ->
6"
4"
2"
-2"
-4"
-6"
Encl. C
Encl. F1
F2
F3
10" pipe
8" pipe
8" pipe
H203
V204
H204
V210
H210
FSEP
M00V
M00H
M00U
2000'
2500'
3000'
3500'
Distance From A0 (ft)

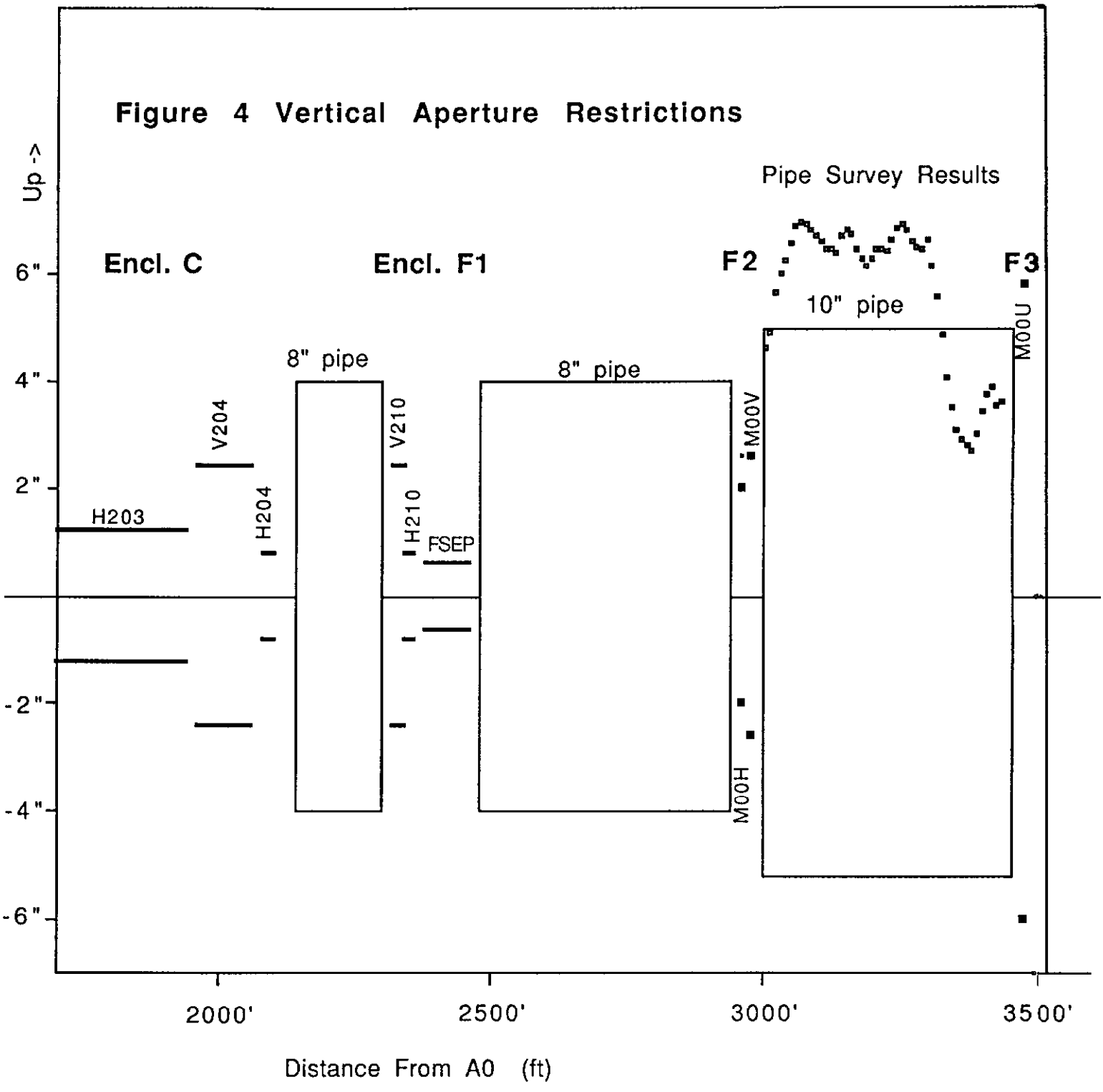
Figure 4 Vertical Aperture Restrictions
Up ->
Pipe Survey Results
Encl. C
Encl. F1
F2
F3
10" pipe
8" pipe
8" pipe
6"
4"
2"
-2"
-4"
-6"
H203
V204
H204
V210
H210
FSEP
M00V
M00H
M00U
2000'
2500'
3000'
3500'
Distance From A0 (ft)

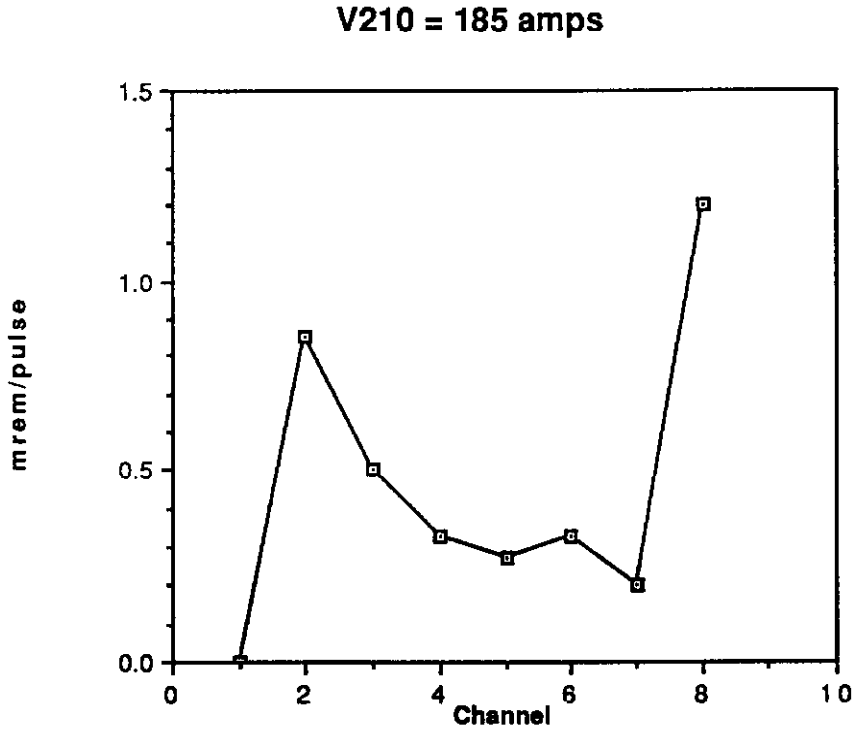

FIGURE 5

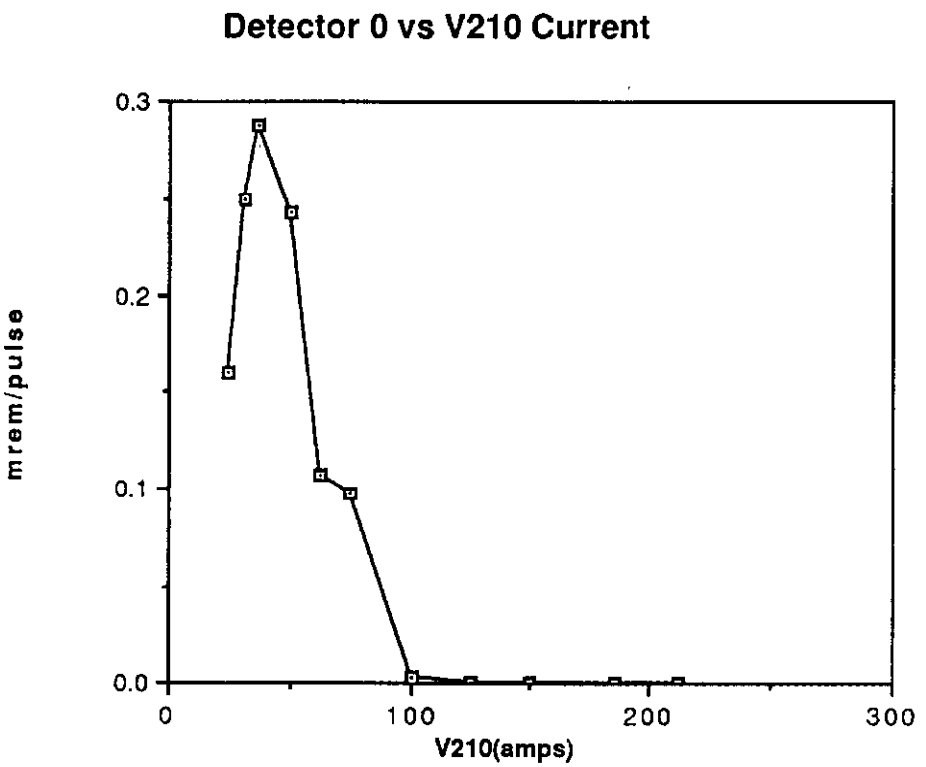

FIGURE 6

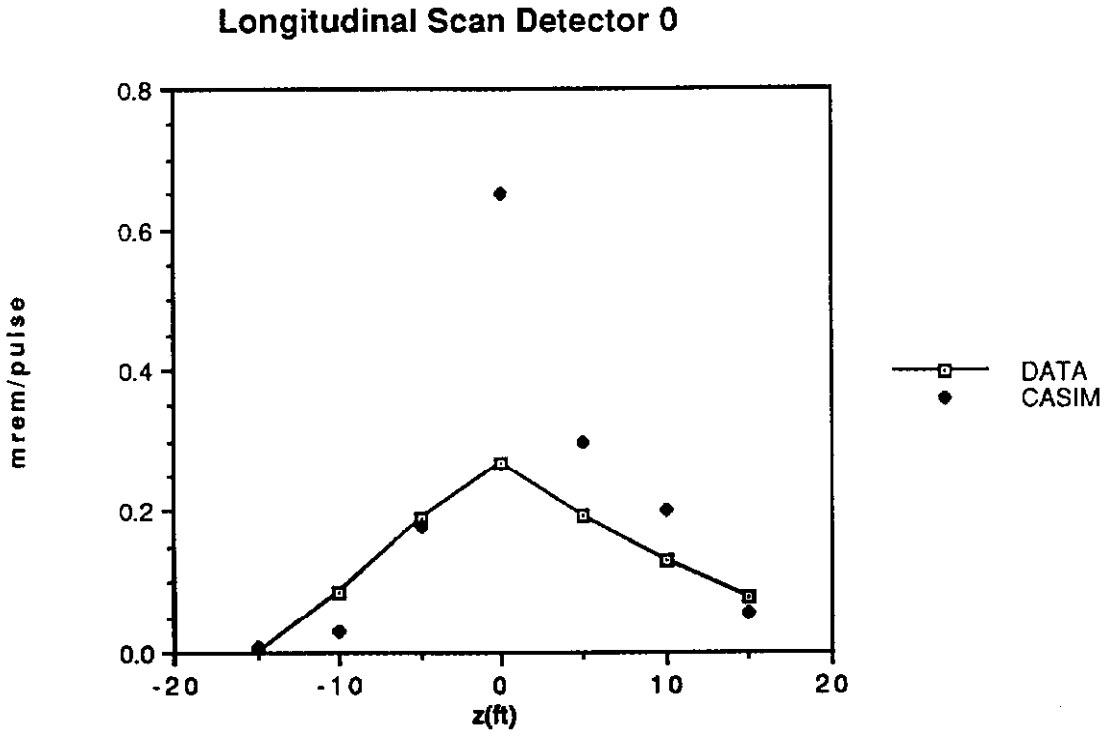

FIGURE 7

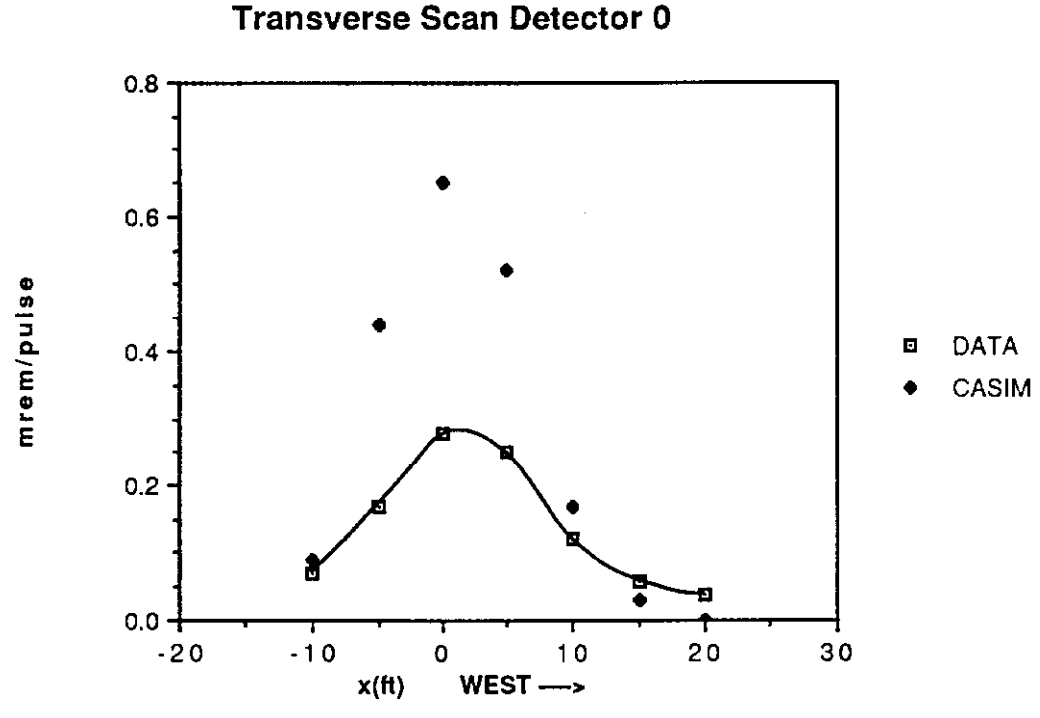

Figure 8

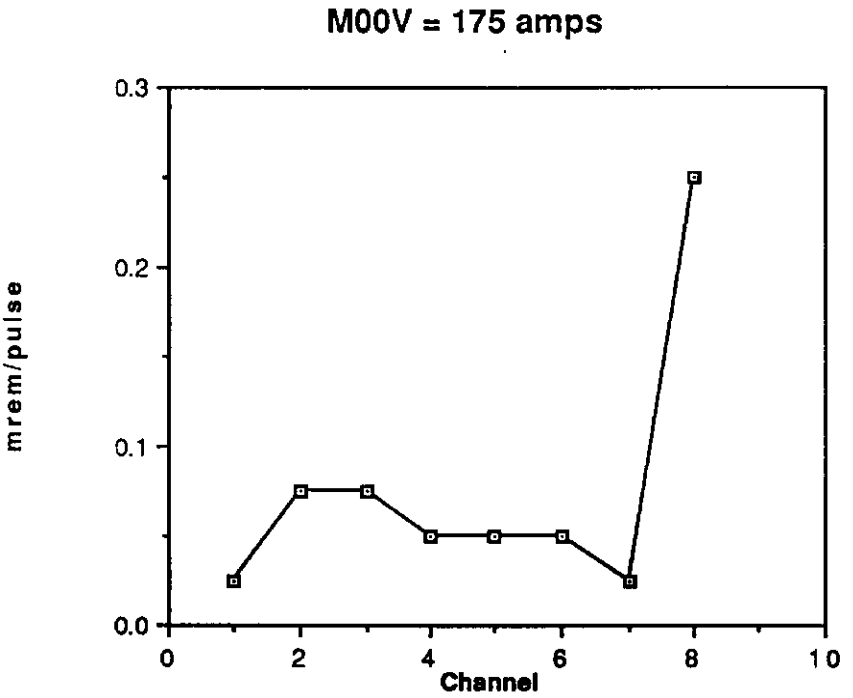

FIGURE 9

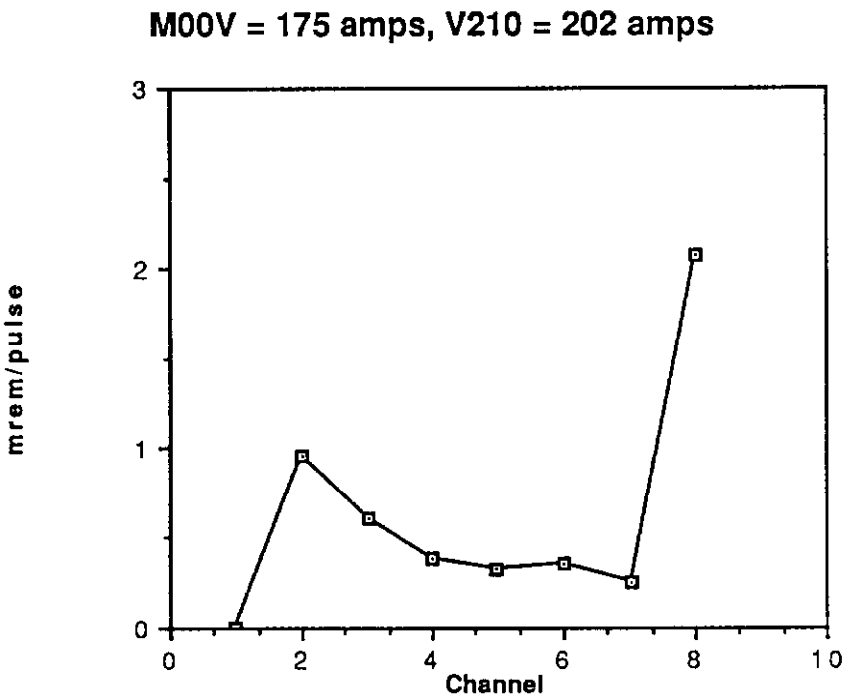

FIGURE 10

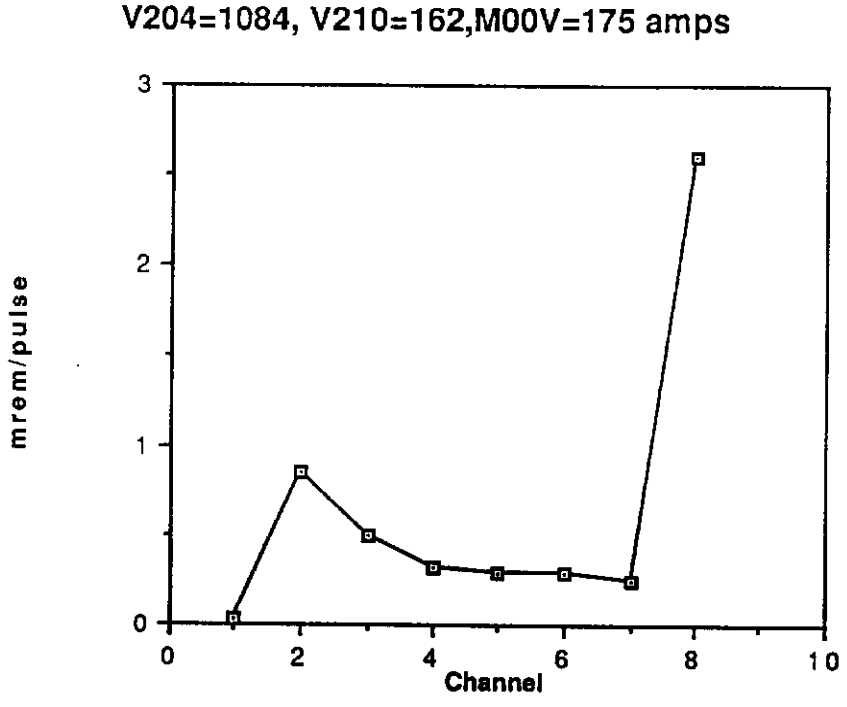

FIGURE 11

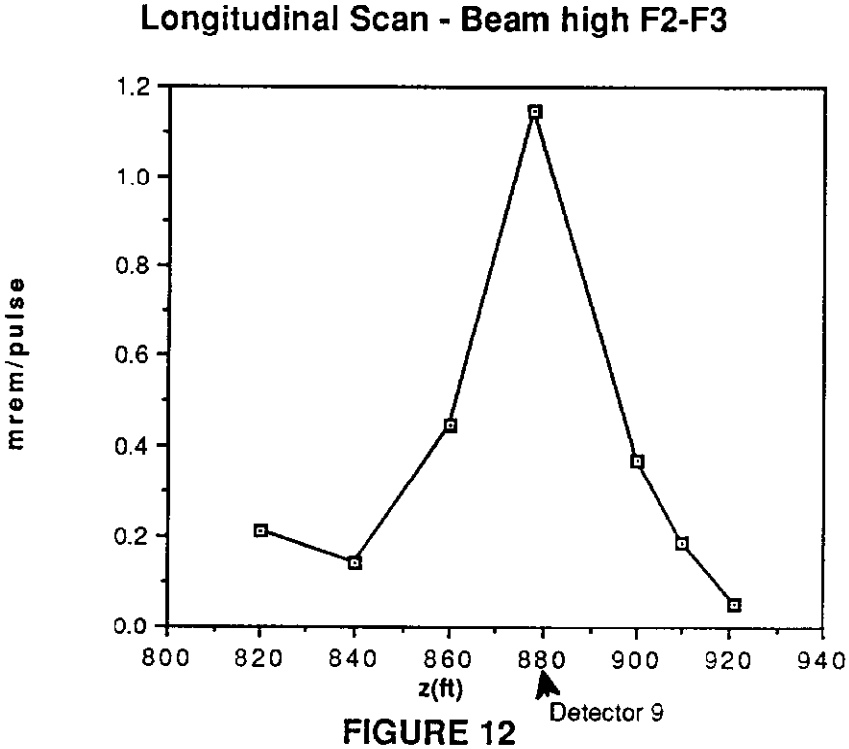

FIGURE 12

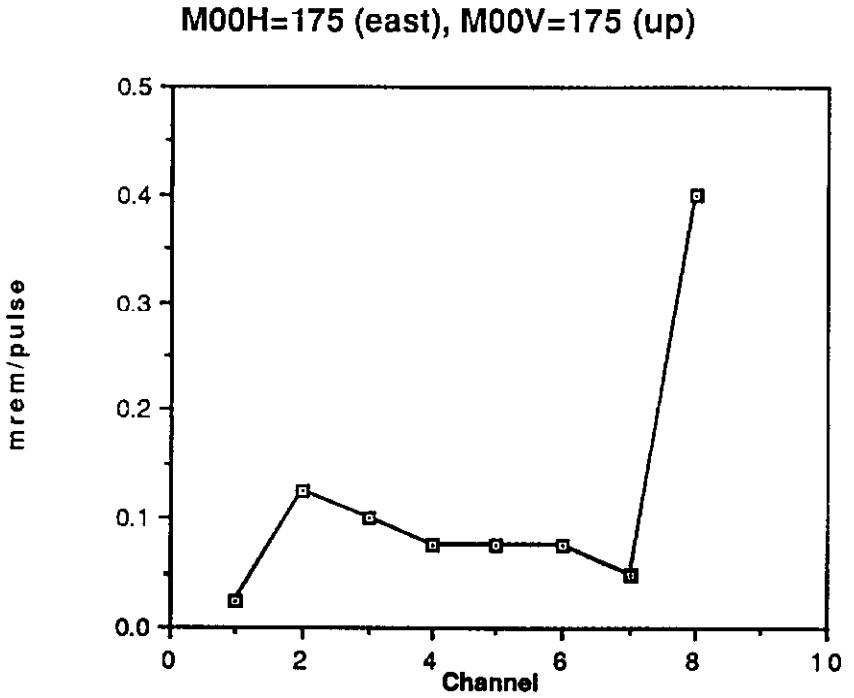

FIGURE 13

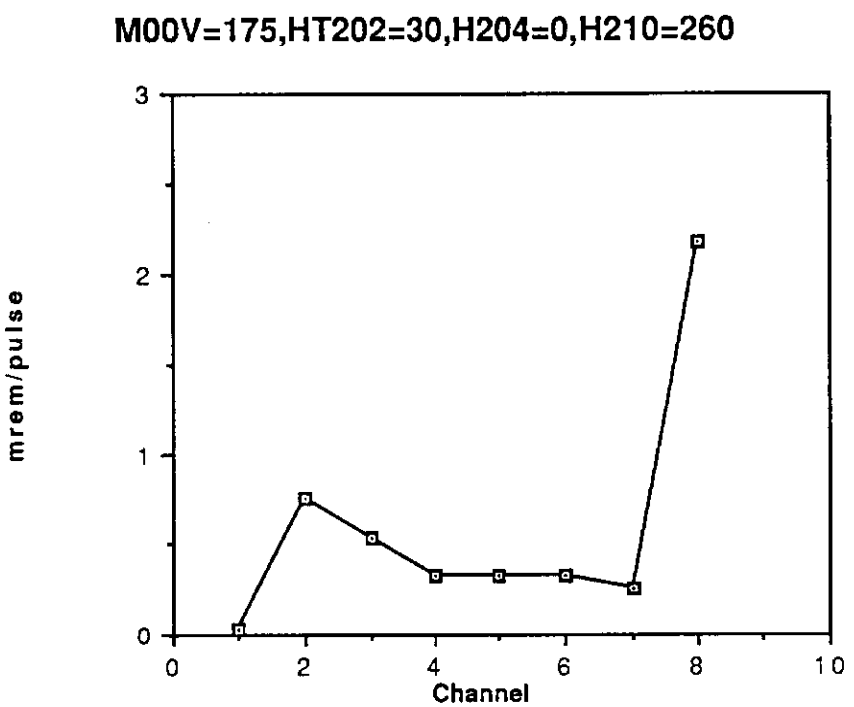

FIGURE 14

Same as Fig.14 except M00H=200(east)

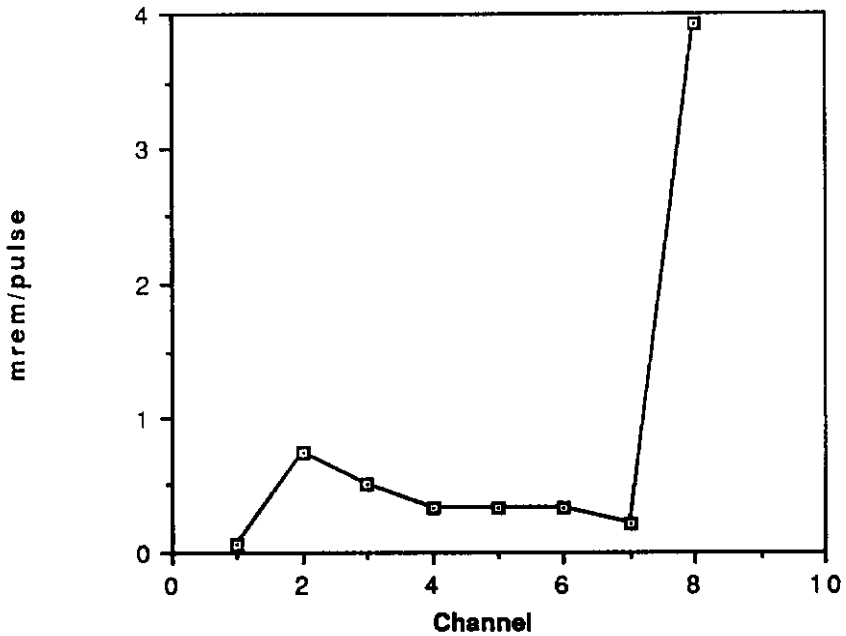

FIGURE 15

Transverse Scan

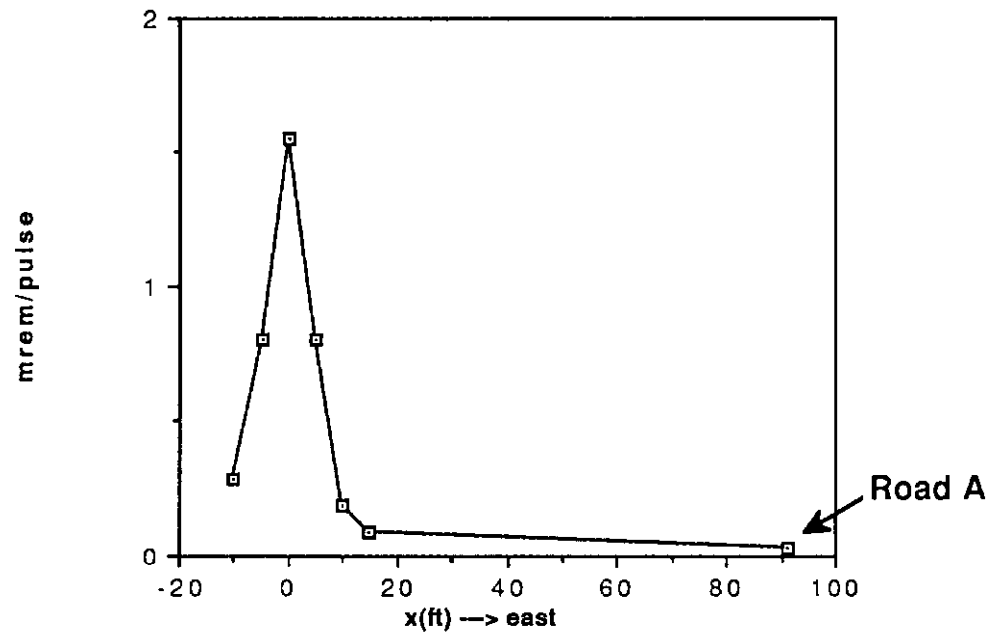

FIGURE 16

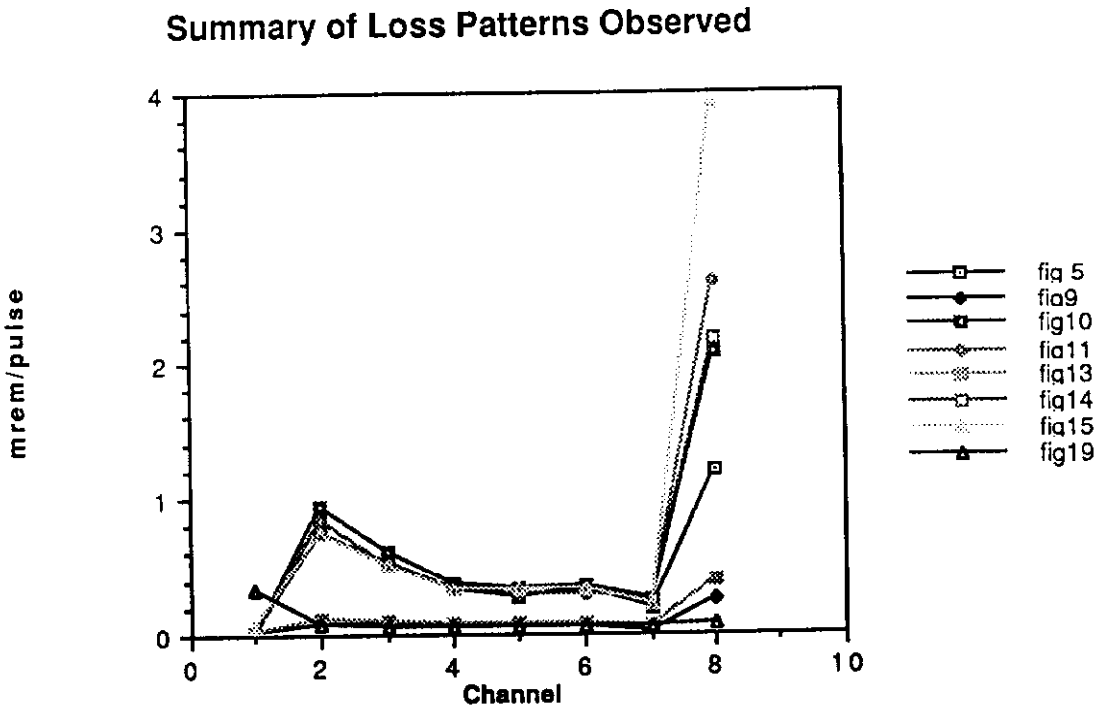

Figure 17

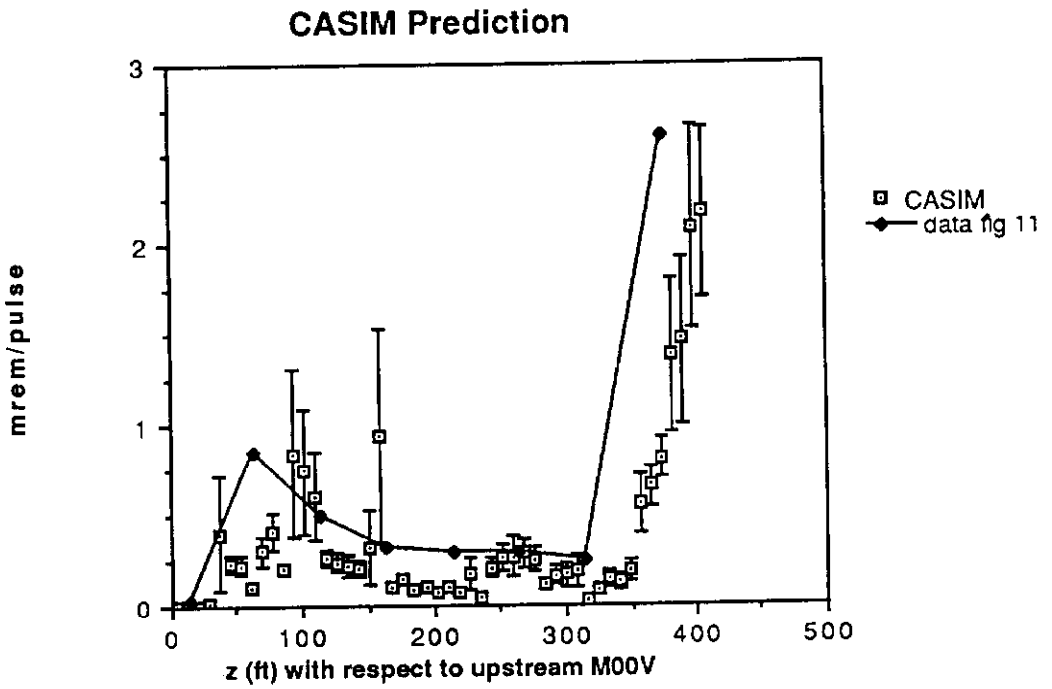

FIGURE 18

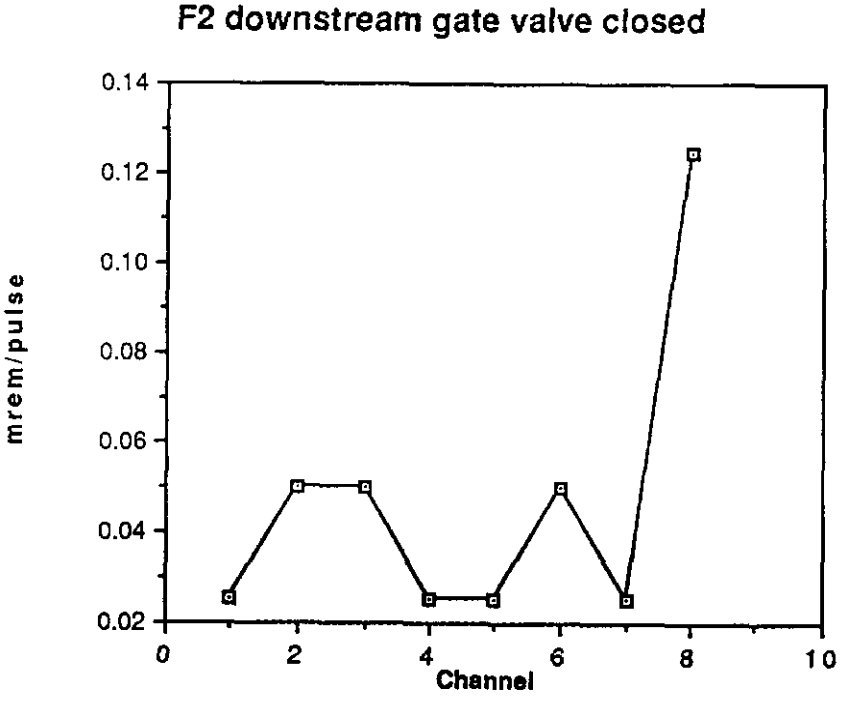

FIGURE 19

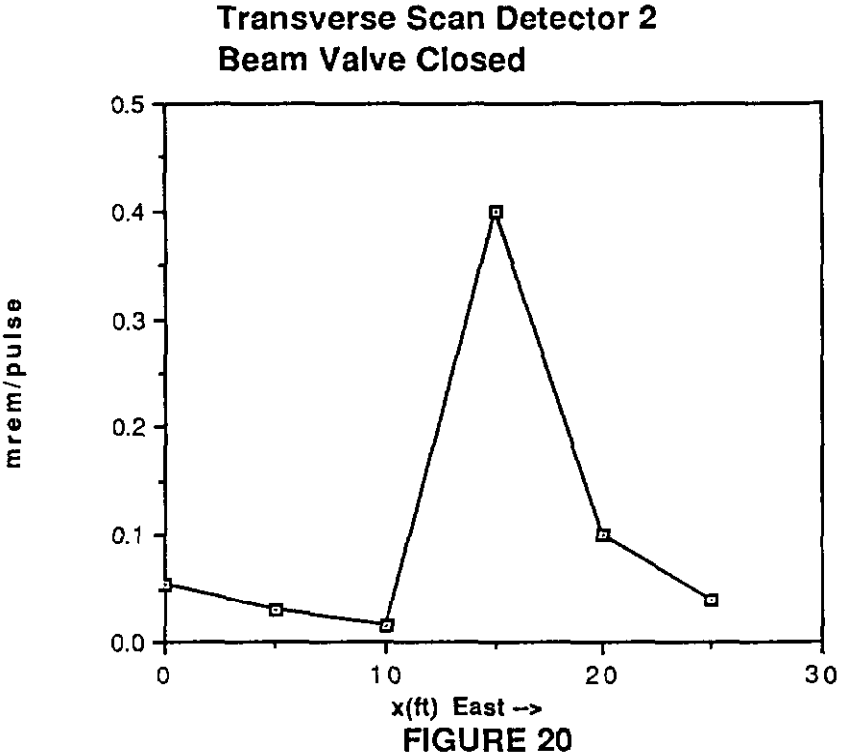

FIGURE 20

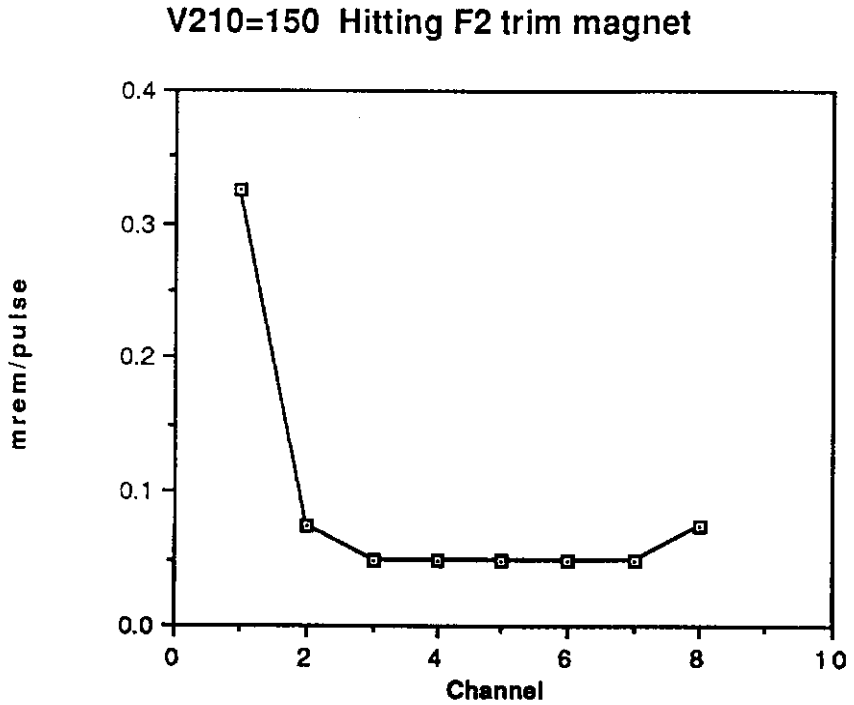

FIGURE 21

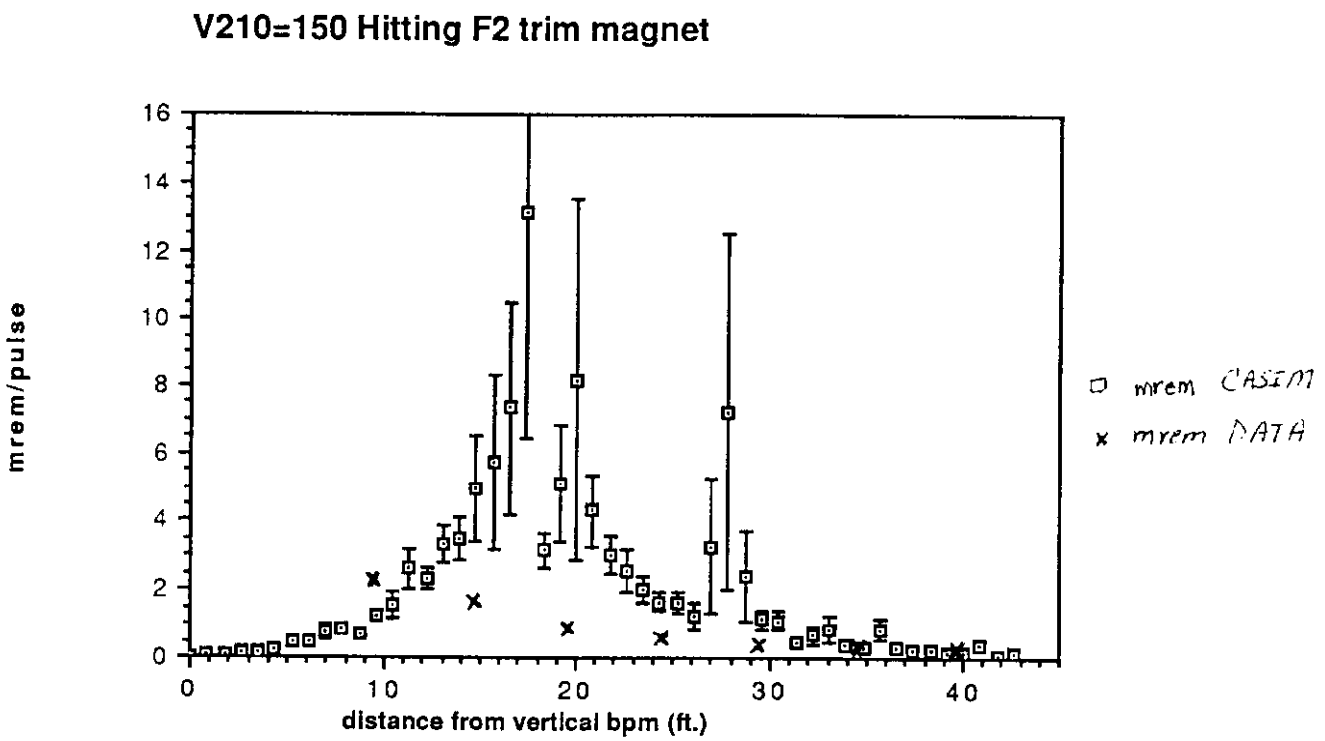

FIGURE 22

Appendix. The figures show the beam trajectories for each of the measurements made. The corresponding tables give the loss monitor and remote radiation monitor data.

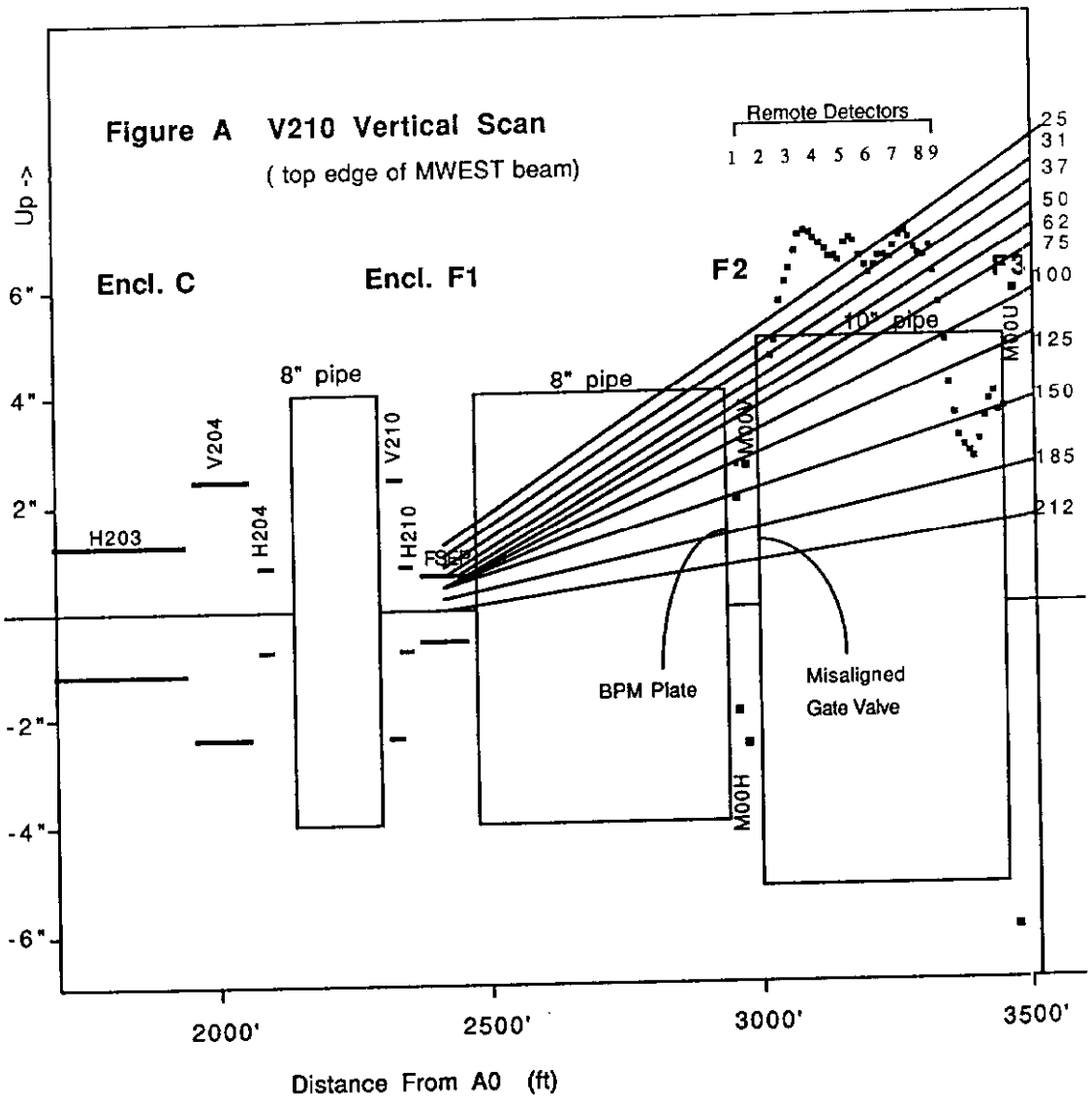

Table A Remote Detectors (25 microrem/count except #0 which is 2.5 microrem/count)

V210	0	2	3	4	5	6	7	9	
212	4	1	1	0	1	1	0	1	
185	4	36	20	12	11	12	9	50	← Nominal tune consistent with beam off background
150	4	2	2	2	1	2	1	3	
125	4	0	0	0	1	1	1	0	
100	4	1	1	1	0	1	1	1	
75	5	1	1	1	1	0	0	0	
62	47	1	1	1	0	0	1	1	
50	100	1	1	1	0	1	1	1	
37	106	0	0	0	0	0	1	1	
31	104	0	0	0	0	1	1	0	
25	68	1	1	1	0	0	0	0	

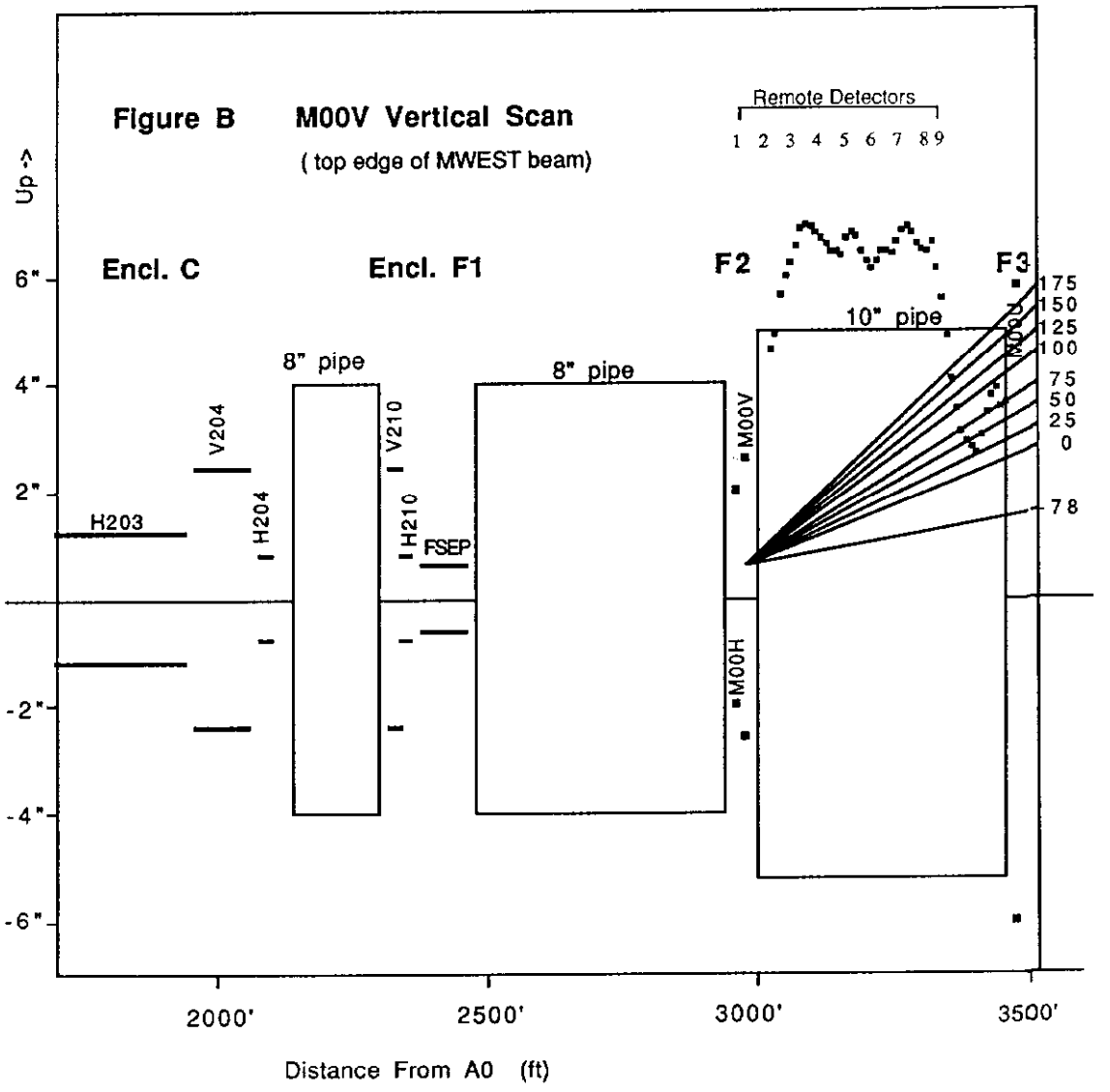

Table B Remote Detectors (25 microrem/count)

M00V	1	2	3	4	5	6	7	9
-78	1	0	1	1	0	0	1	0
0	1	1	1	1	0	1	0	1
25	1	1	0	1	0	0	1	1
50	0	1	0	1	1	1	1	2
75	0	1	1	1	0	1	1	2
100	0	1	2	1	1	1	1	4
125	1	2	2	1	1	1	1	5
150	0	3	2	1	2	2	1	7
175	1	3	3	2	2	2	1	10

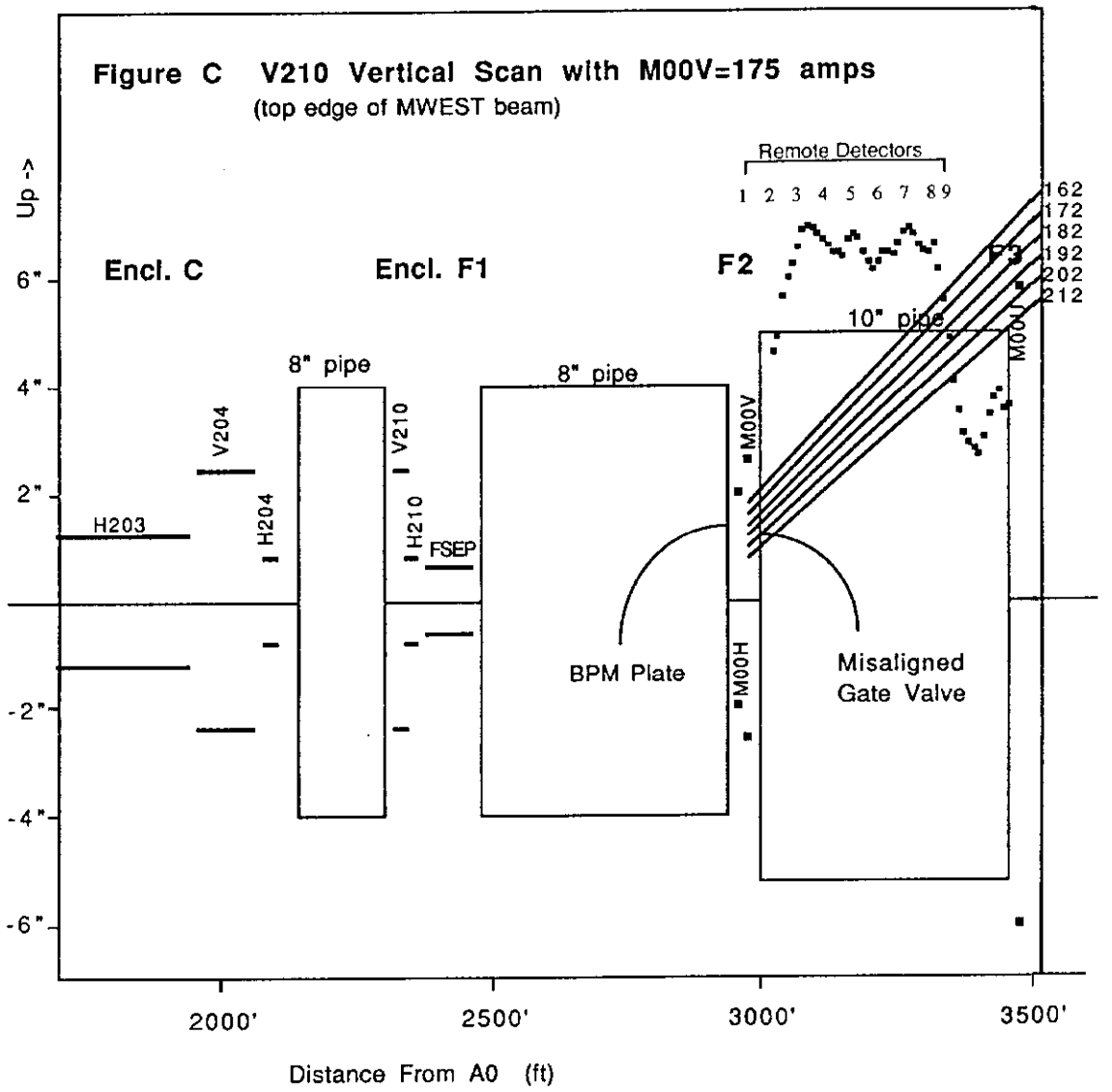

Table C Remote Detectors (25 microrem/count)

Loss Monitors (volts)
Note: 10.2 volts = saturation

V210	1	2	3	4	5	6	7	9	F2US	M00H	M00V	F2DS	F3US	M00U	F3DS
212	1	5	3	2	2	3	2	13	10.2	0.1	0.1	6.0	0.0	10.2	10.2
202	0	38	24	15	13	14	10	83	1.9	0.9	0.9	10.2	0.0	10.2	6.8
192	6	23	15	9	8	8	6	46	0.6	10.2	10.2	10.2	0.2	10.2	1.6
182	3	36	21	11	9	10	7	73	0.6	1.8	1.8	10.2	0.1	10.2	1.4
172	16	27	17	9	7	4	4	23	0.1	10.2	10.2	10.2	5.5	5.5	0.3
162	16	4	3	4	4	3	2	2	0.2	10.2	10.2	10.2	10.2	1.0	0.1

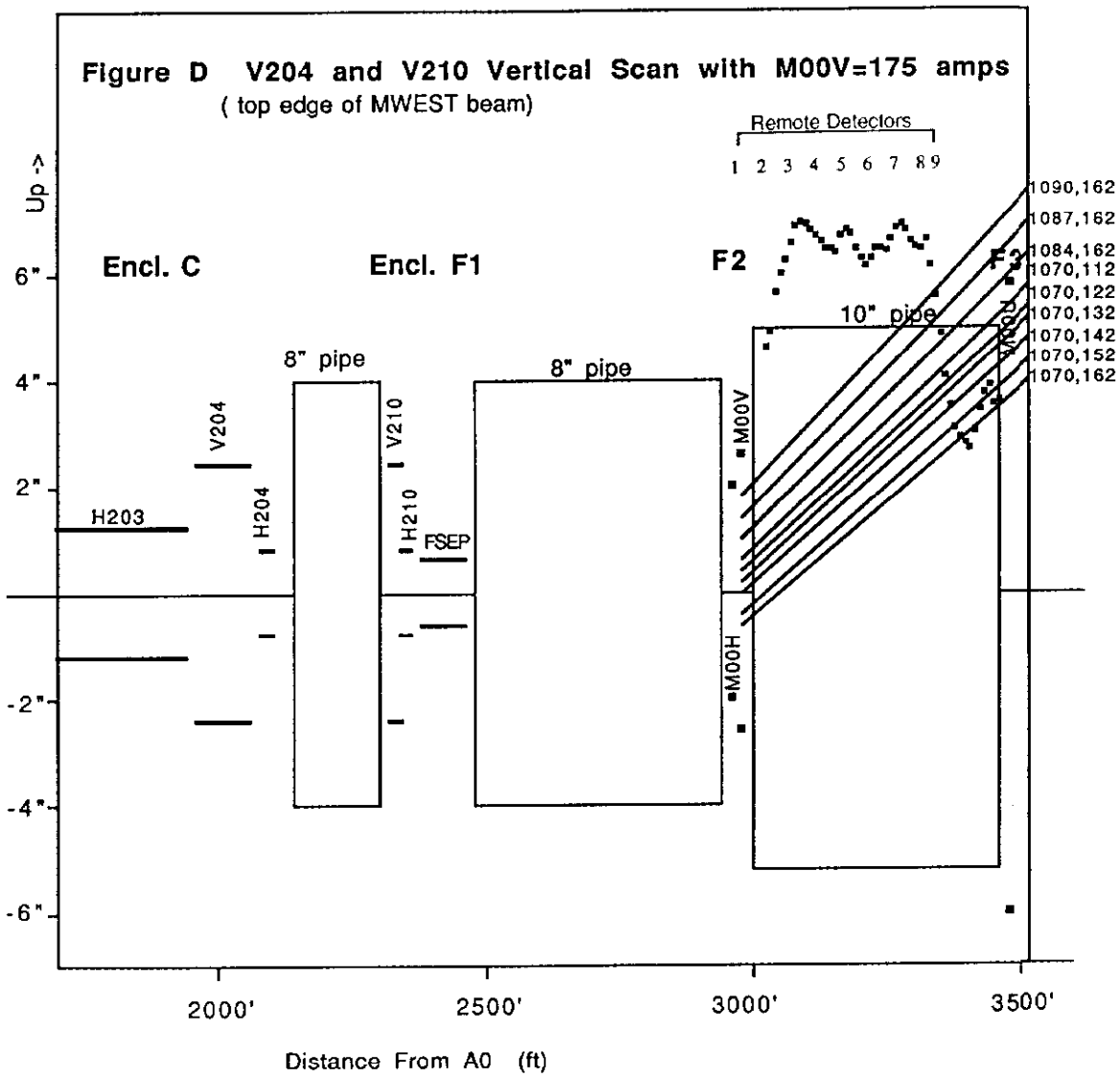

Table D Remote Detectors (25 microrem/count) Loss Monitors (volts) Note: 10.2 volts = saturation

V204	V210	1	2	3	4	5	6	7	9	F2US	M00H	M00V	F2DS	F3US	M00U	F3DS
1090	162	16	4	3	4	4	3	2	2	0.0	10.2	10.2	10.2	10.2	1.0	0.0
1087	162	12	31	19	9	8	7	4	24	0.1	10.2	10.2	10.2	1.4	5.9	0.2
1084	162	1	34	20	13	12	12	10	104	0.9	10.2	10.2	10.2	0.1	10.2	2.2
1070	112	3	30	18	11	10	11	8	78	0.8	10.2	10.2	10.2	0.1	10.2	1.7
1070	122	1	38	22	14	12	15	11	89	1.8	0.7	0.7	10.2	0.0	10.2	4.1
1070	132	1	2	1	1	0	1	1	5	10.2	0.4	0.4	1.7	0.0	10.2	6.4
1070	142	1	0	0	1	1	0	0	0	8.5	0.4	0.4	0.2	0.0	10.2	10.2
1070	152	0	0	0	0	0	1	1	1	6.3	0.3	0.3	0.1	0.0	10.2	10.2
1070	162	1	1	0	0	0	0	0	0	10.2	0.3	0.3	0.1	0.0	10.2	10.2

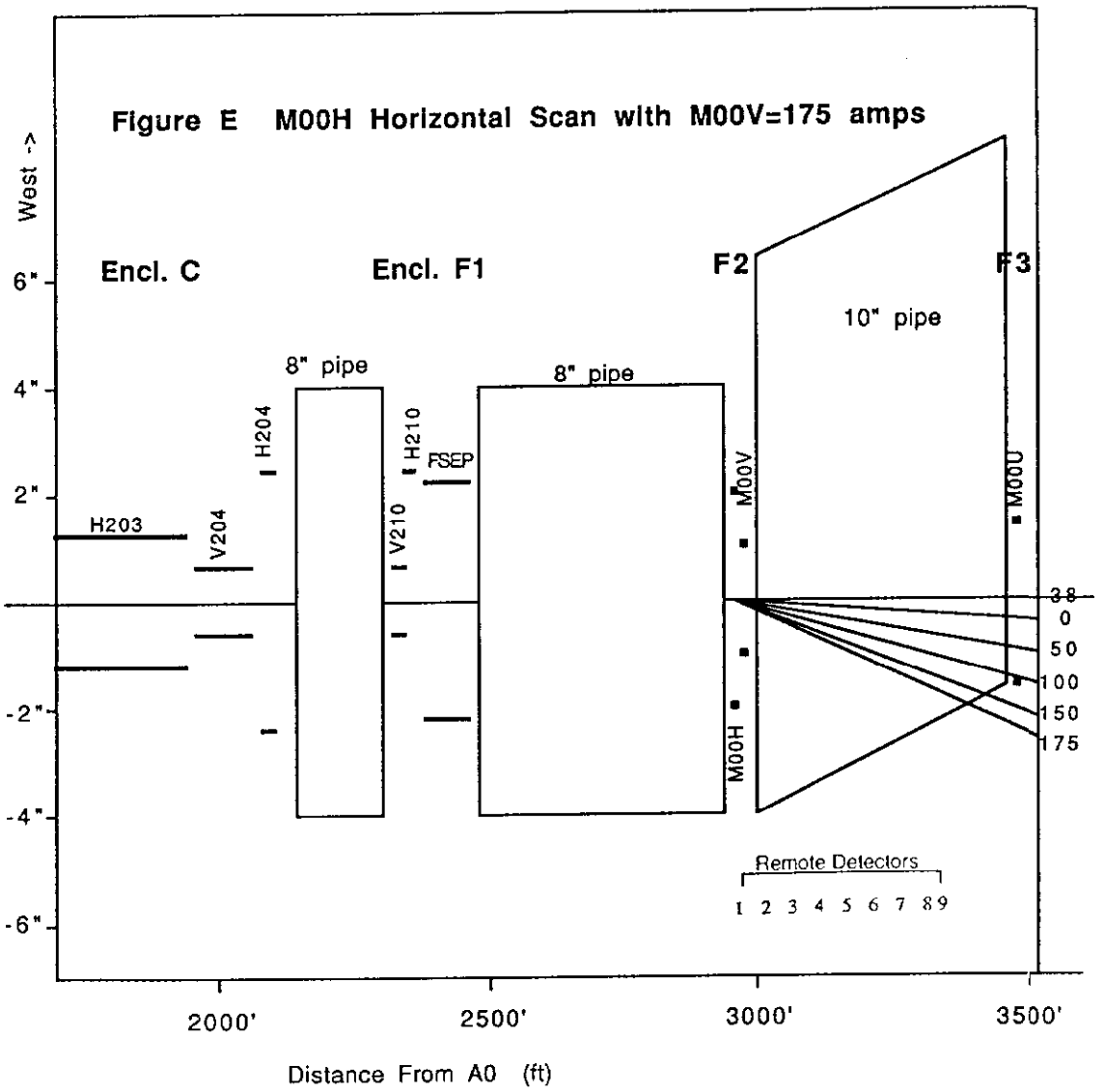

TABLE E Remote Detectors (25 microrem/count) Loss Monitors (volts) note: 10.2 volts = saturation

M00V	1	2	3	4	5	6	7	9	F2US	M00H	M00V	F2DS	F3US	M00U	F3DS
-38	1	4	2	2	1	2	2	10	10.2	0.4	0.4	4.4	0.0	10.2	10.2
0	1	4	2	1	2	2	2	10	9.7	0.4	0.4	4.7	0.0	10.2	7.7
50	1	3	3	2	2	2	2	12	10.2	0.4	0.4	5.1	0.0	10.2	5.1
100	1	4	4	2	2	2	2	13	10.2	0.4	0.4	6.3	0.0	10.2	5.4
150	0	6	3	3	3	3	3	16	10.2	0.4	0.4	7.1	0.0	10.2	5.5
175	0	5	4	3	3	3	2	16	9.7	0.4	0.4	7.6	0.0	10.2	5.3

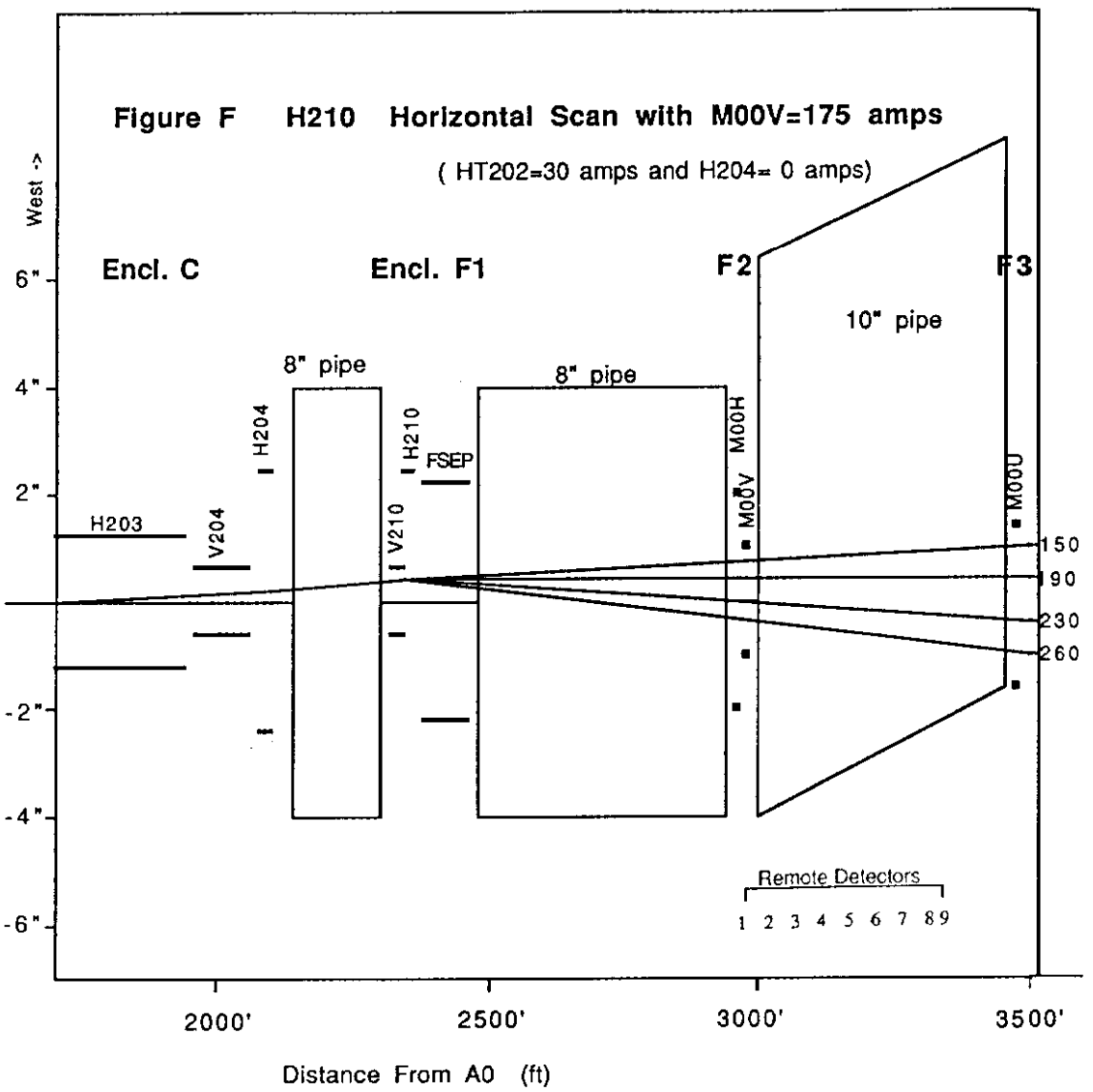

TABLE F Remote Detectors (25 microrem/count) — Loss Monitors (volts) note: 10.2 volts = saturation

H210	1	2	3	4	5	6	7	9	F2US	M00H	M00V	F2DS	F3US	M00U	F3DS
160	1	1	1	1	1	1	1	3	10.2	0.5	0.5	1.2	0.0	10.2	10.2
180	1	5	3	3	3	3	2	15	9.5	0.5	0.5	1.4	0.0	10.2	5.8
190	1	12	8	5	4	5	4	29	8.3	0.4	0.4	1.5	0.0	10.2	6.6
200	1	20	13	8	7	9	7	47	6.7	0.4	0.4	8.2	0.0	10.2	7.2
210	0	27	18	11	9	11	8	63	6.5	0.5	0.5	10.2	0.0	10.2	6.9
220	0	30	21	12	12	13	10	76	5.0	0.5	0.5	10.2	0.0	10.2	7.1
230	1	32	22	14	12	14	10	86	3.6	0.5	0.5	10.2	0.0	10.2	6.5
240	1	30	21	13	12	14	10	87	3.3	0.5	0.5	10.2	0.0	10.2	5.9
250	1	30	21	13	13	14	10	88	3.2	0.5	0.6	10.2	0.0	10.2	5.3
260	1	30	21	13	13	13	10	87	3.0	0.6	0.8	10.2	0.0	10.2	4.8

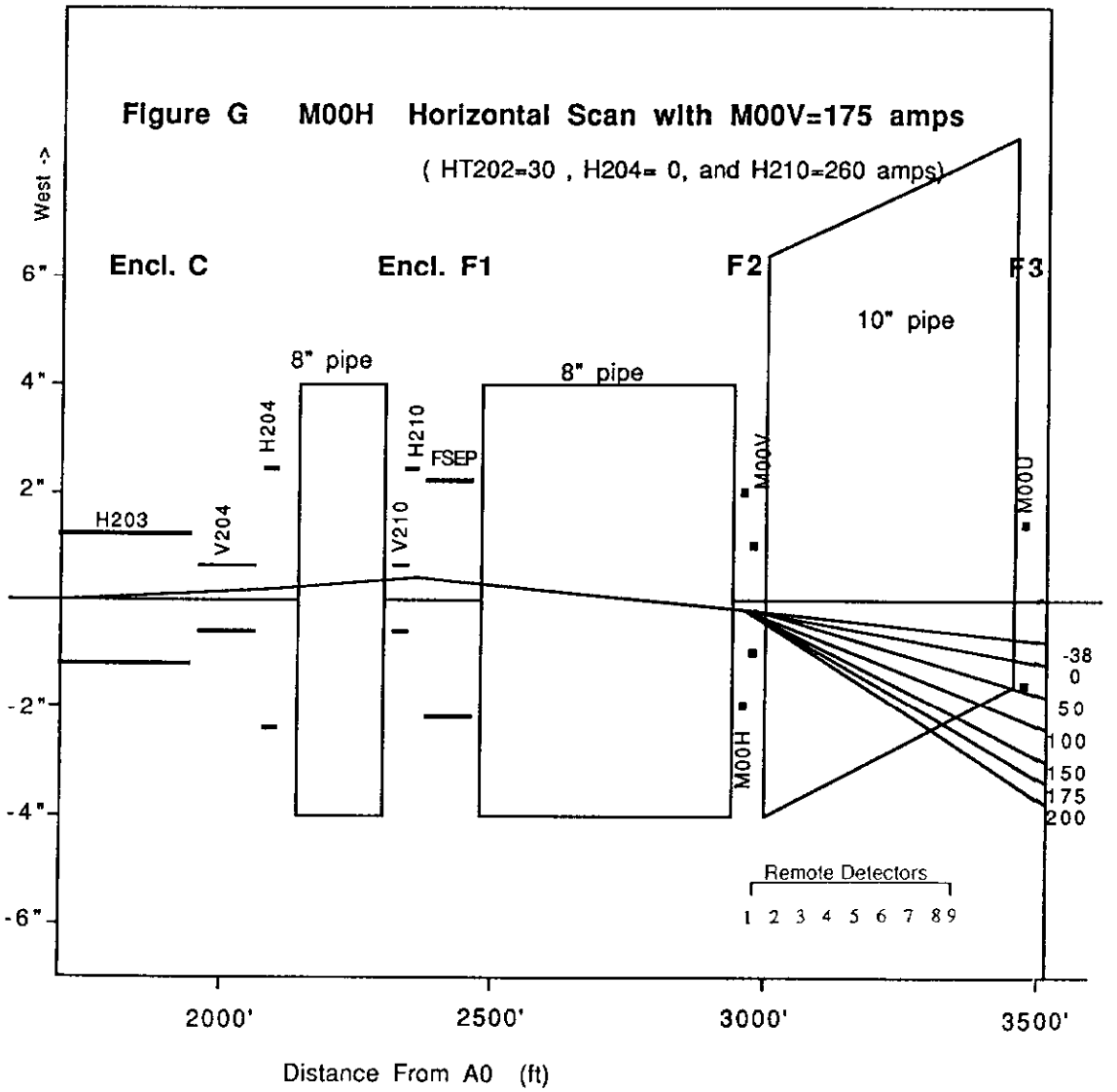

Table G Remote Detectors (25 microrem/count) Loss Monitors (volts) Note: 10.2 volts = saturation

M00H	1	2	3	4	5	6	7	9	F2US	M00H	M00V	F2DS	F3US	M00U	F3DS
-38	1	30	21	13	13	13	10	87	3.0	0.6	0.8	10.2	0.0	10.2	4.8
50	2	26	18	12	11	11	8	86	2.0	0.9	2.0	10.2	0.0	10.2	3.0
75	2	29	20	12	12	13	9	97	1.9	0.9	1.9	10.2	0.0	10.2	2.8
100	2	30	20	13	12	12	9	102	1.8	0.8	1.9	10.2	0.0	10.2	2.6
125	2	30	21	13	13	13	10	112	1.8	0.9	1.9	10.2	0.0	10.2	2.5
150	1	27	18	12	12	12	9	110	1.6	0.8	1.8	10.2	0.0	10.2	2.3
175	2	29	20	13	12	12	10	137	1.6	0.9	1.9	10.2	0.0	10.2	2.2
200	2	30	20	13	13	13	9	157	1.5	0.8	1.9	10.2	0.0	10.2	2.0

Table H Remote Detectors (25 microrem/count)

Loss Monitors (volts)
Note: 10.2 volts = saturation

Beam Valve Closure Test

1	2	3	4	5	6	7	9	F2US	M00H	M00V	F2DS	F3US	M00U	F3DS
1	2	2	1	1	2	1	5	0.1	0.4	0.4	0.7	0.1	6.6	0.8
0	2	1	1	1	1	1	4	0.1	0.4	0.4	0.7	0.1	6.6	0.8

Beam Loss on M00H Magnet in F2

1	2	3	4	5	6	7	9	F2US	M00H	M00V	F2DS	F3US	M00U	F3DS
13	3	2	2	2	2	2	3	0.0	10.2	10.2	10.2	10.2	0.9	0.0